RESULTS AND DISCUSSION (III)

Crystal Structures of Myosin II Catalytic Domains Reveal a Large Rotation in the Converter Domain

In the available crystal structures myosin II, S1 adopts two major conformations[7,9,11,12]. These conformations are believed to represent the putative "prestroke" and "poststroke" states in an ATPase cycle (Figure 3). The superimposed structures reveal that the biggest changes occur in the so called "converter domain", which according to the crystal structures undergoes a 90° rotation from the putative pre- to poststroke state[15]. The magnitude of this rotation would indeed be enough to pivot the lever arm resulting in a step size of about 5 - 10 nm as it has been measured in single molecule optical trapping experiments[79,80].

To follow the predicted rotation of the converter domain in real time, the present work aimed to develop a single molecule fluorescence anisotropy assay. Following the anisotropy change of a fluorophore in single molecule experiment was successfully applied to the myosin V protein[42]. The anisotropy change of a rigidly attached fluorophore to a protein reports directly on the rotational motion of this protein domain. Because rigid attachment of the fluorescent dye to the protein is necessary, a novel fluorescent dye called FlAsH, was used to label the converter domain of the single headed *Dictyostelium discoideum* myosin II S1[81]. FlAsH binds to four cysteines and is thus rigidly attached to the protein. In addition, FlAsH binds very specifically to a CCXXCC motif with XX being any amino acid except cysteines. Thus this approach makes deletion of wild type cysteines unnecessary in the protein of interest. In the original paper, FlAsH was claimed to bind specifically to a CCXXCC sequence in an α-helix[81,82]. To label the *Dictyostelium discoideum* myosin S1 with the FlAsH dye, two different mutants were expressed with a CCXXCC motif introduced into an α-helix in the converter domain. As discussed below, extensive attempts to label both mutant myosin II S1 proteins with the FlAsH dye remained unsuccessful. However, during the course of

labeling attempts the myosin II S1 heavy chain was discovered unexpectedly to interact with the regulatory light chain (RLC) domain.

Protein Design and Purification

To label the converter domain with the FlAsH dye, two mutant myosin S1 proteins in *Dictyostelium discoideum* were expressed. In each mutant, four solvent exposed residues (D724, A725, K728, H729 and L751, A752, E755, E756) in an α-helix of the converter domain were mutated to cysteines via QuikChange site-directed mutagenesis. To facilitate QuikChange mutagenesis, the myosin II heavy chain in the pTIKL OE plasmid (>12 kb) was sub-cloned into the pBluescript sK^+ plasmid (2900 kb) using the Xba I and the Nco I unique restriction sites. The mutated heavy chain gene was cloned back into the pTILK OE plasmid and the mutated protein was expressed in AX3-Orf^+ cells. The protein expression levels of both mutants (M-724 and M-751 hereafter) were indistinguishable from the wild type protein.

Wild type and Mutant Myosin II S1 Protein Purification

The $(His)_6$ tagged myosin II S1 proteins were FPLC purified first by Ni-NTA affinity chromatography followed by a MonoQ™ ion exchange chromatography. Figure 56 shows an example of the M-751 purification.

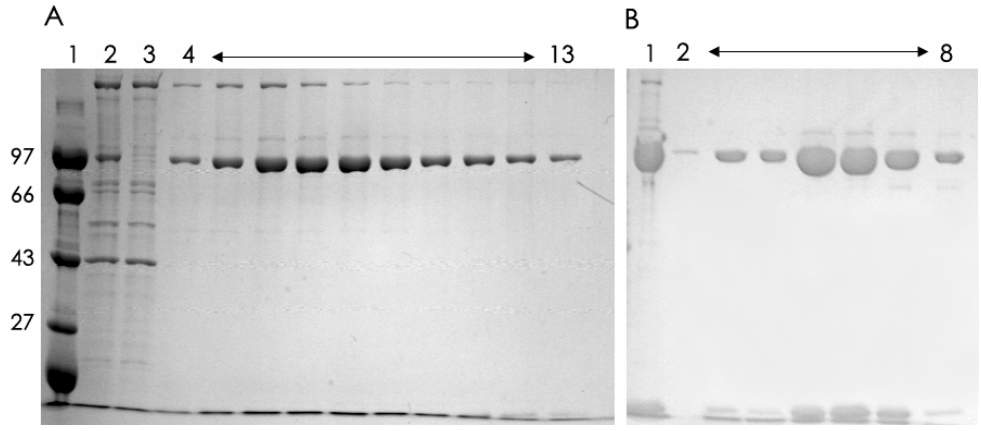

Figure 56: (A) FPLC purification of the M-751 protein on a Ni-NTA column. Lane 1: marker, Lane 2: loaded protein, Lane 3: flow through, Lane 4 – Lane 13: elution profile from the Ni-NTA column (10% SDS-polyacrylamide gel). **(B)** M-751 protein purification on the MonoQ column. Lanes 1: column load, Lane 2-Lane 8: elution profile from the MonoQ column (10% SDS-polyacrylamide gel).

Actin Activated ATPase of the Mutant Myosin II S1 Proteins

The introduction of mutant cysteines into the converter domain did not alter the actin activated ATPase activity of the mutant proteins compared to the wild type myosin II S1 (Figure 57, Table 3).

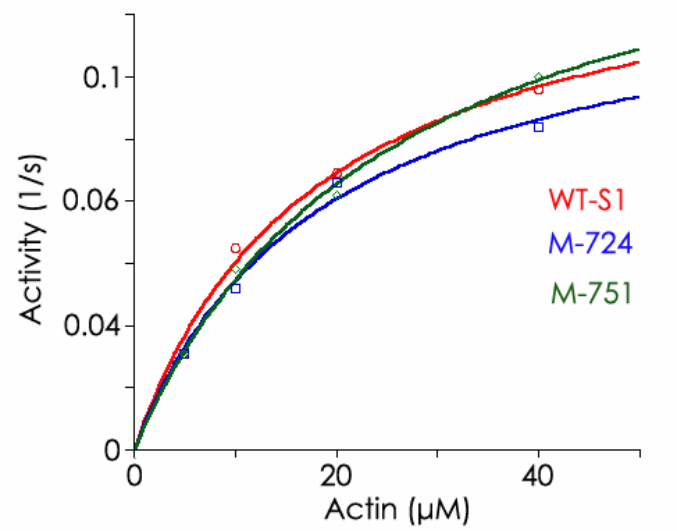

Figure 57: Actin activated ATPase of wild type myosin S1 (WT-S1), M-751, and M-724. The mutated proteins displayed identical actin activated activities as the wild type myosin II S1. The data are fit to the equation v_{max}*[Actin]/(K_M+[Actin]) to obtain the steady-state kinetic parameters.

Table 3: Calculated values of v_{max} and K_M

	WT-S1	M-751	M-724
v_{max} (s^{-1})	0.17 ± 0.017	0.19 ± 0.017	0.17 ± 0.016
K_M (μM)	18.2 ± 4.1	25.8 ± 4.3	18.7 ± 4.2

FlAsH Labeling of the M-751 and M-724 Myosin II S1 Constructs

Extensive attempts to label the mutant myosin S1 proteins with the FlAsH dye remained unsuccessful. Figure 58 shows a typical example of labeled mutant proteins M-724 and M-751 containing the CCXXCC motifs along with the wild type myosin II S1 as a negative control. The CCXXCC motifs that were introduced into the helices did not show more labeling than the wild type control. This particular reaction was carried out at room temperature for 2 hours (pH 7.4) with a protein to dye ratio of (1:5).

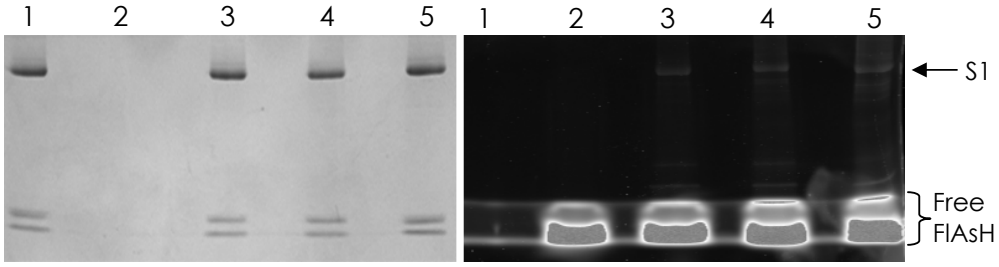

Figure 58: (**left**) Coomassie stained SDS-polyacrylamide gel showing the FlAsH labeling of the wild type and the mutant myosin II S1. Lane 1: wild type myosin II S1, 2: FlAsH dye, Lane 3: FlAsH labeled M-751, Lane 4: FlAsH labeled M-724, Lane 5: FlAsH labeled wild type S1. (**right**) Fluorescent scan of the same SDS-polyacrylamide gel.

To ensure that the experimental conditions were appropriate for FlAsH dye labeling, a bacterially expressed kinesin protein (K339) was labeled as a positive control[83]. K339 was C-terminally fused to a 17 amino acid long sequence (WEAAAREACCRECCARA) containing the CCRECC motif showed extensive labeling (Figure 59). In a recent publication by the Tsien group, the authors conclude that FlAsH binding forces the peptide sequence into a hairpin and that binding is not compatible with an α-helix as initially described[73]. It is conceivable that both helices chosen for labeling in the converter domain were not flexible enough to allow hairpin formation, which would explain the failed labeling attempts. On the other hand, the kinesin protein that was used as positive control showed extensive labeling because the CCXXCC motif was introduced as a C-terminal tag which is presumably flexible enough to adopt a hairpin structure (Figure 59).

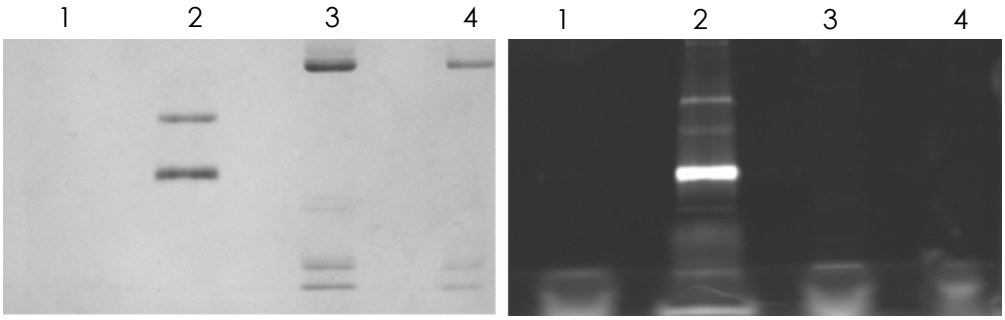

Figure 59: (**left**) Coomassie stained SDS-polyacrylamide gel. Lane 1: FlAsH dye, Lane 2: FlAsH labeled K339 kinesin, Lane 3: FlAsH labeled M-751, Lane 4: FlAsH labeled M-724. (**right**) Fluorescent scan of the same SDS-polyacrylamide gel.

The HC and the RLC can Interact in Solution

During the course of the labeling attempts it was discovered that in standard ATPase buffer an up-shifting in denaturing SDS-PAGE of the myosin II S1 band occurred both for the wild type and the mutant proteins (Figure 60). This up-shifting was dependent on the presence of 2,3-dimercapto-1-propane-sulfonic acid (DMPS) which is used in the labeling reaction as a FlAsH-activator. The up-shifting was quantitatively reversible upon addition of excess DTT. This data suggested that a covalent crosslink is formed between two cysteines in myosin S1 leading to an altered mobility in denaturing SDS-PAGE. DMPS presumably functions as a crosslinker because it contains two thiol groups that can be oxidized over the labeling time course by molecular oxygen.

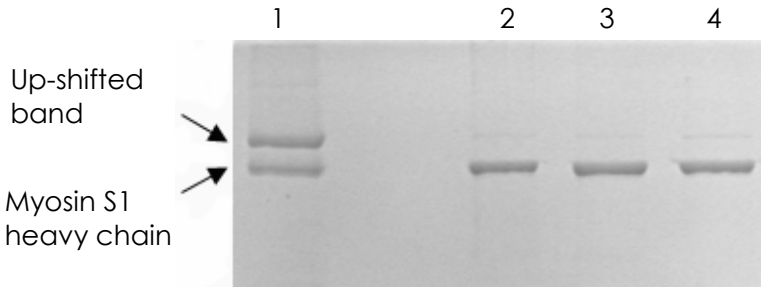

Figure 60: Up-shifted band of the coomassie stained M-751protein in the presence of DMPS. The up-shifting is reversed after adding excess DTT (10 mM). Lane 1: Crosslinked M-751 in the presence of 0.1 mM DMPS, Lane 2: Crosslinked M-751 after addition of excess DTT, Lane 3: Crosslinked M-724 after addition of excess DTT, Lane 4: Crosslinked wild type myosin S1 after addition of excess DTT.

To further characterize the up-shifted band, Mass Spectrometry (MS2) was applied to identify the involved proteins. Briefly, the protein containing fractions or selectively cut coomassie stained protein bands were digested with a proteolytic enzyme. The protein fragments were separated via HPLC and the masses of the peptides were determined by mass spectrometry (MS1). The subsequent fragmentation of the separated peptides yielded their masses (MS2). The peptide fragments are identified by appropriate software that can match the found masses with protein data bases.

The MS2 data obtained from selectively cut S1 heavy chain and up-shifted coomassie gel bands showed that the up-shifted band contained the RLC of myosin S1 which was absent in the lower myosin II S1 heavy chain band (Figure 61).

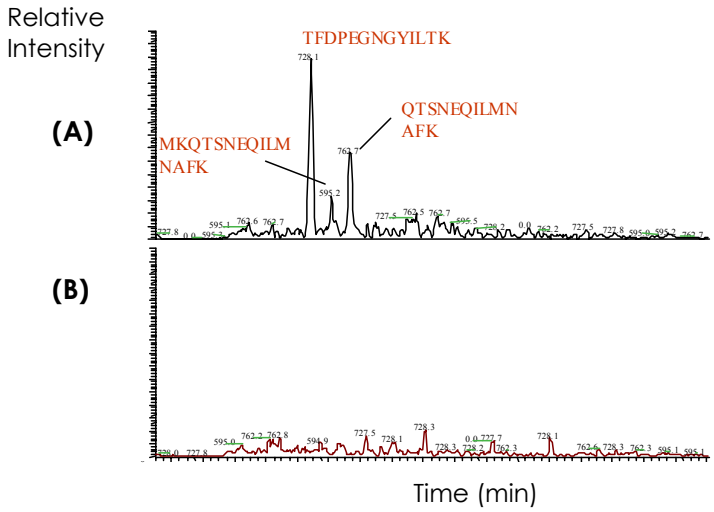

Figure 61: (A) MS/MS data for the up-shifted band shows RLC peptides in addition to peptides of the HC. The detected RLC peptides are shown in red. **(B)** The RLC peptides are absent in the myosin HC coomassie band.

A covalent crosslinking between the RLC and the HC in myosin S1 was unexpected because the RLC contains only one cysteine (C49) which is roughly 90 Å apart from the closest cysteine in the HC in the crystal structure (Figure 62). The observed crosslinking however suggests that in solution this cysteine of the RLC at least temporarily comes close to one of the cysteines in the HC.

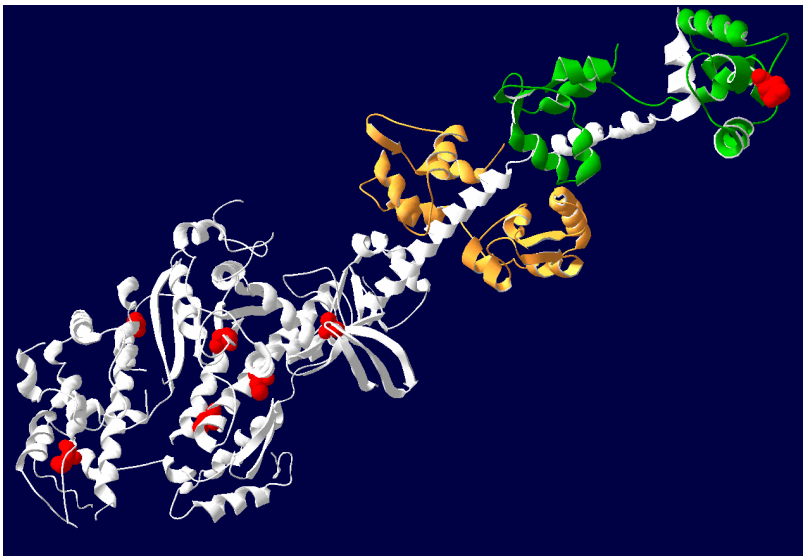

Figure 62: The myosin II S1 crystal structure from scallop in the nucleotide free state (1FDL). Positions in the crystal structure that correspond to cysteines in *Dictyostelium* myosin II are marked red. The distance between the cysteine C49 in the RLC (green) and the closest cysteine in the HC (white) is 97 Å. The heavy chain is shown in white, ELC in yellow and RLC in green.

Characterization of the RLC-HC-Interaction

Crosslinking Between RLC and HC Occurs Intramolecularly

Before further exploring the biochemical nature of the RLC-HC interaction, it was critical to demonstrate that the observed RLC-HC interaction is occurring intramolecularly and not intermolecularly. An intermolecular crosslinking between the RLC of one myosin S1 to another HC should yield a protein complex, which has twice the size of the myosin II S1. In a Superdex 200 (HR 10/30) gel-filtration column no differences in the elution profile of the crosslinked and wild type myosin II S1 could be detected (Figure 63). The identical elution profiles of the uncrosslinked and the over 90% crosslinked protein on the gel filtration column suggested that the crosslinking of the RLC and HC did not occur between two myosin S1 molecules.

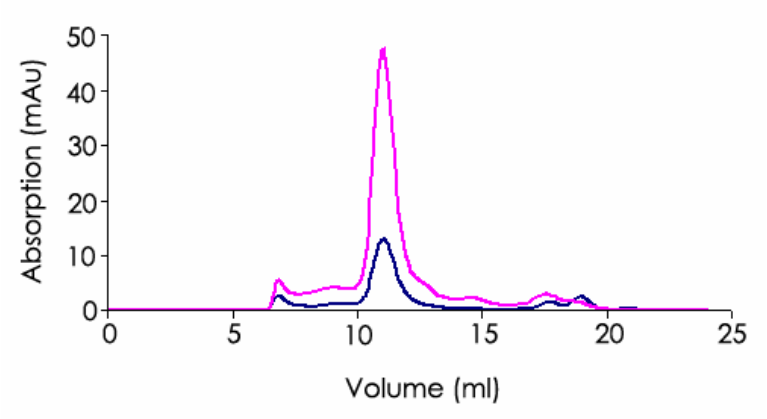

Figure 63: Superdex 200 (HR 10/30) Gel filtration chromatography of crosslinked (blue) and uncrosslinked (pink) myosin S1. Uncrosslinked and crosslinked myosin S1 have identical elution profiles with the uncrosslinked S1 eluting at 11.04 ml and the crosslinked S1 eluting at 11.06 ml. The difference in the UV intensity of the crosslinked vs. uncrosslinked S1 is due to different amount of protein loaded onto the gel filtration column.

Crosslinking of RLC and HC is Nucleotide State Dependent

The crosslinking between RLC and the HC was nucleotide state dependent (Figure 64). ATP seemed to be required for crosslinking while no crosslinking can be detected in the absence of nucleotides. A pre-incubation of the protein prior the crosslinking reaction with 0.5 mM DTT was critical for the specific nucleotide state dependent crosslinking. The presence of other nucleotides such as ADP and ADP*VO_4 also lead to crosslinking (not shown).

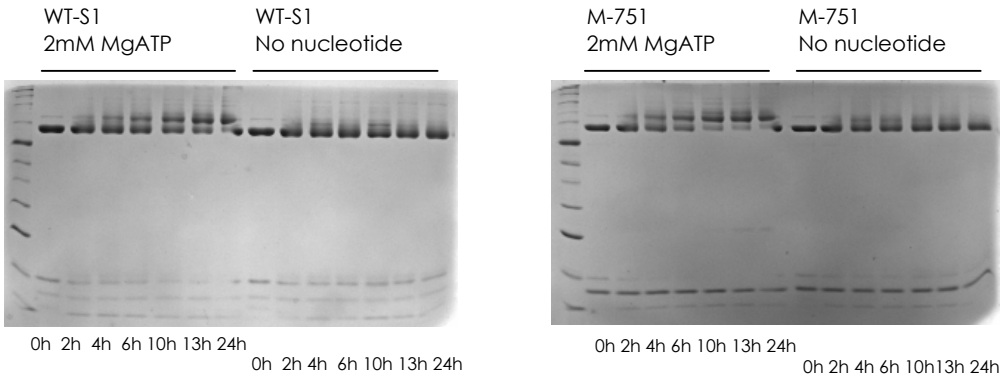

Figure 64: (Left) Time courses of the crosslinking reactions in the presence and absence of ATP with the wild type (WT-S1) myosin II S1. **(Right)** Time courses of the crosslinking reactions in the presence and absence of ATP with the mutant (M-751) myosin II S1.

Possible explanations for the absolute requirement for nucleotides would be that myosin adopts a different conformation in presence of nucleotides placing the head closer to the RLC. Alternatively, the mobility of the lever arm is increased resulting in a higher probability for the RLC to crosslink to the HC. A third explanation is that a cysteine in the HC becomes more exposed or reactive upon nucleotide binding, which in turn allows crosslinking.

Characterization of the Crosslinking Cysteines in RLC and HC via Cysteine Footprinting

To identify the crosslinking cysteine(s) on the HC to the single cysteine on the RLC, footprinting experiments were carried out with two different probes: N-(iodoacetyl, *p*-chlorobenzyl)-glucamide (ICAT) (Figure 65) and 2-nitro-5-thiocyanobenzoic acid (NTCB), a cysteine specific cutting reagent (Figure 73). The mechanism of cysteine footprinting using ICAT and NTCB is discussed below.

Cysteine footprinting via ICAT labeling

ICAT reagent (**3**) was synthesized from N-*p*-cholorobenzyl-glucamine (**1**) and iodoacetamide (**2**), and used to specifically label the crosslinked cysteines (Figure 65). The free cysteines in the crosslinked protein were reacted with excess iodoacetamide to block any unspecific reactions with the ICAT reagent. A subsequent reduction of the crosslinked cysteines using DTT allowed the specific labeling of the crosslinked cysteines with the ICAT reagent. The protein was then digested using the trypsin proteolytic enzyme. The digested protein fragments were batch bound to a custom made boronate column (a kind gift from Pehr Harbury, Stanford University). The sugar moiety on the ICAT molecule allowed the purification of the ICAT tagged peptides over the boronate column. The obtained peptides were analyzed via MS2 spectrometry. The recovered peptides poorly matched the theoretically calculated peptide masses (not shown). This was presumably largely due to the unspecific binding of the peptides to the boronate resin. Furthermore, the overall coverage of peptides with the MS2 technique is dependent on the

instrumentation and the mobility of the peptides were generally low (30 - 40%). It is conceivable that peptides containing the ICAT reagent were not detectable due to their lacking mobility in the electrical field.

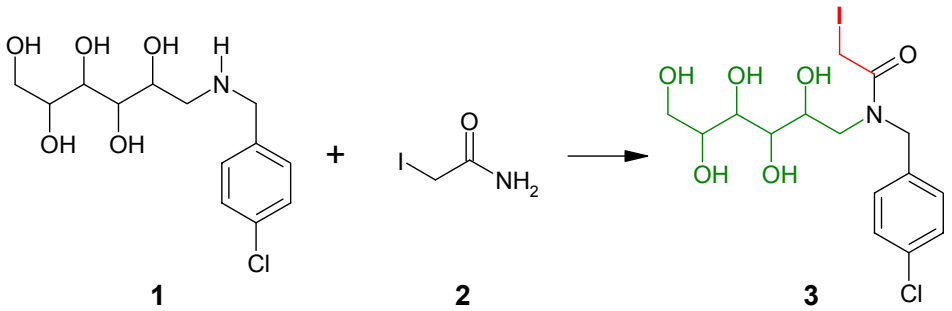

Figure 65: One step synthesis of N-(iodoacetyl, *p*-chlorobenzly)-glucamide (**3**). The cysteine reactive moiety is shown in red and the affinity tag for boronate column purification is shown in green, respectively.

Cysteine Footprinting via NTCB Labeling

The reaction of the NTCB reagent (Figure 73) with cysteine residues leads to a specific digestion pattern with hydroxyl ions at the NTCB modified cysteine residue. This fact was exploited to probe the differences in the digestion pattern of the crosslinked and uncrosslinked M-751 protein. Similar to the cysteine foot printing using the ICAT reagent, the crosslinked and the uncrosslinked proteins were denatured and reacted with iodoacetamide to saturate the solvent exposed cysteines. The reaction was then quenched with excess βME which also reduced the crosslinked cysteines. Thus the crosslinked cysteines remained unlabeled by iodoacetamide. The reaction product was denatured with an 8M GuHCl along with the NTCB reagent. All exposed cysteines were labeled with NTCB and cleaved in basic 10 M urea. The cleavage products were characterized by MS2 spectrometry. The identified peptides of the crosslinked mutant and wild type protein via MS2 spectrometry for the most part did not match the calculated masses based on the expected theoretical cleavage patterns. This was probably due to miscleavage of the protein and to the generally low coverage of peptides in MS2 spectrometry as explained above.

A conclusive analysis of the crosslinking cysteine in the heavy chain with the single cysteine in the regulatory light chain requires a single cysteine mutant of the myosin S1 heavy chain. Promising candidates would be the solvent exposed cysteines and the reactive SH2 (C678), respectively. More importantly, to show that the crosslinking of a cysteine on the RLC with spatially distant cysteine(s) in the catalytic domain is not an artifact due to the unconstrained neck in the myosin S1 construct, a similar analysis of a myosin II construct containing the S1/S2 junction is required to show that the RLC is indeed coming close to the catalytic domain during an ATPase cycle. A possible candidate for this analysis would be the HMM construct because it contains the S1/S2 junction and it does not form thick filaments due to its truncated tail domain (Figure 1).

Myosin Light Chain Kinase-A Expression and Purification

To investigate the effect of RLC phosphorylation, myosin light chain kinase-A (MLCK-A) was expressed and purified to quantitatively phosphorylate the RLC[72]. The MLCK-A construct is mutated at the residue T166 to glutamate (T166E). The T166E mutant mimics the phosphorylated state of the MLCK-A and displays a 12-fold higher enzyme activity[72]. The phosphorylation state of the RLC was followed by urea-glycerol gel electrophoresis because the phosphorylation modifies the mobility of the RLC protein. In all experiments, quantitative phosphorylation or dephosphorylation of the RLC at the beginning and at the end of the experiment was confirmed by urea-glycerol gels (Figure 66).

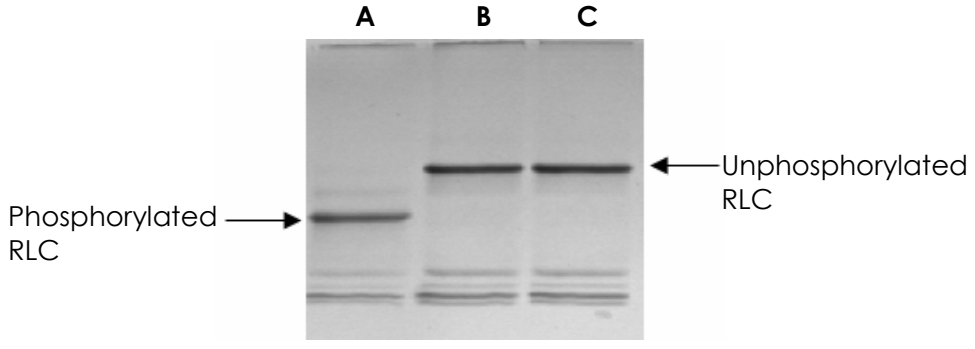

Figure 66: Phosphorylation of RLC caused a higher electrophoretic mobility in the urea-glycerol-gel. **(A)** Quantitatively phosphorylated RLC of the wt myosin II S1 sample treated with MLCK-A. **(B)** Quantitatively dephosphorylated RLC using alkaline phosphatase **(C)** untreated RLC.

The RLC Phosphorylation Inhibits the RLC - HC Interaction

The RLC in *Dictyostelium* myosin II exerts its role in a phosphorylation state dependent manner[17]. To investigate the dependence of crosslinking on the RLC phosphorylation state, the RLC was quantitatively phosphorylated with purified MLCK-A[72,84]. While in the presence of ATP crosslinking of the unphosphorylated RLC was >90%, the crosslinking of the phosphorylated RLC was inhibited upto 40% in the presence of ATP after 24 hours (Figure 67).

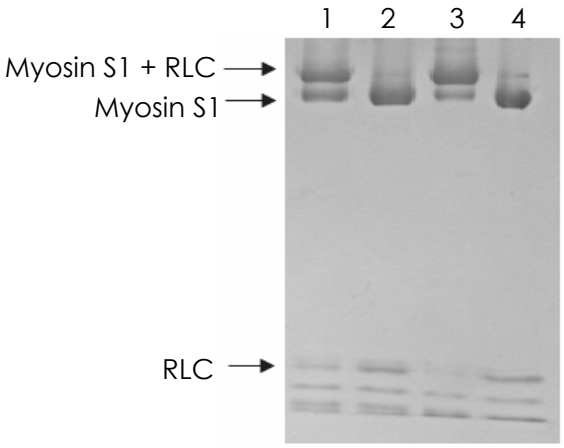

Figure 67: Phosphorylation state dependent crosslinking of the wild type S1 protein after 24 hours. Lane 1: phosphorylated RLC/+DMPS, Lane 2: phosphorylated RLC/-DMPS, Lane 3: unphosphorylated RLC/+DMPS, Lane 4: unphosphorylated RLC/-DMPS. The depletion of the RLC by crosslinking was also apparent in this gel.

This result suggests of that the RLC spends on average more time close to cysteines of the heavy chain if the RLC is unphosphorylated. Possible models would be that the RLC binding domain is more flexible if the RLC is unphosphorylated so that the HC and RLC come into contact more often or that dephosphorylation induces global conformational changes within the protein, decreasing the distance between the cysteine of the RLC and the cysteine in the HC.

Small Angle X-ray Scattering (SAXS) experiments were performed to further explore if RLC phosphorylation induces a global conformational change. SAXS is sensitive to global conformational of a protein. The radius of gyration (R_g) can be calculated from the SAXS data which is a measure of a proximate size of the molecule. To investigate a phosphorylation state dependent

conformational change in the myosin S1 protein, the wild type *Dictyostelium* myosin II S1 was quantitatively phosphorylated and unphosphorylated as previously described. No phosphorylation state dependent change of the global protein conformation was detected by this technique (Figure 68). However, the absence of a detectable difference in the SAXS profiles upon RLC phosphorylation cannot be taken as evidence that no conformational change is taking place because the signal difference if any is expected to be small. This is because the mass of the lever arm is small compared to the head. Also, SAXS would not necessarily report on an increased mobility of the lever arm because on time average the conformations of phosphorylated and unphosphorylated S1 might be similar.

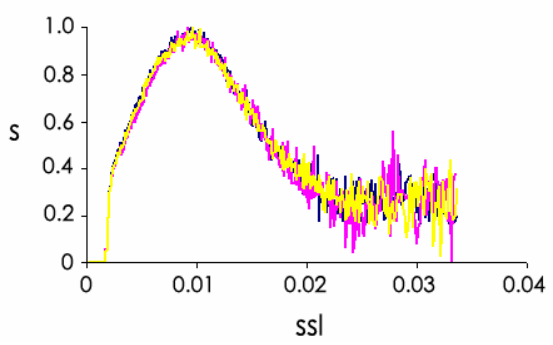

Figure 68: Normalized Kratky plots of the *Dictyostelium* myosin II. Phosphorylated myosin II S1 in the presence of ATP resulted in a R_g value of 55.9 (+/-0.5) and in the absence of ATP a R_g value of 56.1 (+/- 0.6), respectively. In the presence of ATP unphosphorylated myosin II S1 the R_g value was 54.9 (+/-0.5).

Role of RLC Phosphorylation in Dictyostelium Myosin II

The phosphorylation state dependent crosslinking data suggests that upon RLC dephosphorylation the "neck" and the "head" come closer on average over time, resulting in higher crosslinking efficiency. This suggests that in solution the protein is on average more "bent" in the unphosphorylated state.

As discussed above, the dephosphorylation of smooth muscle myosin seems to induce a bent conformation in one head resulting in head-head interactions which was proposed to affect the actin activated ATPase activity (Figure 5)[24,25]. Furthermore, in a very recent study site-directed spin labeling revealed a conformational switch in the phosphorylation domain of the smooth muscle

myosin II under physiological conditions[85]. The N-terminal phosphorylation domain in the RLC showed a disorder-to-order transition upon phosphorylation. This transition in turn was coupled to conformational changes that caused decreased head-head interactions. According to this model, the RLC phosphorylation frees constrained heads leading to an enhanced interaction with the actin filaments. As the smooth muscle myosin II, the *Dictyostelium* myosin II actin activated ATPase is also regulated by phosphorylation of an N-terminal serine residue[86,87]. Thus, a similar conformational change could take place upon dephosphorylation of the RLC in *Dictyostelium* myosin II which would be consistent with our data. Biochemical data show that the actin activated ATPase activity of the *Dictyostelium* full-length myosin II is increased 6-fold upon RLC phosphorylation, whereas the myosin S1 is not regulated[17,69]. The presented model provides explanations why single headed myosin S1 is not regulated by the RLC phosphorylation: no head-head interactions can be formed in the single headed S1 and free S1 heads are sterically much less constrained than myosin heads, which are in the context of thick filaments. Thus, a bending of S1 heads in the unphosphorylated state would not result in an inhibition of myosin-actin interactions.